JOURNAL OF MATERIALS SCIENCE 30 (1995) 2145–2152

Effects of surfactants on the precipitation and properties of colloidal particles from forced hydrolysis of $FeCl_3$–HCl solution

K. KANDORI, I. HORII, A. YASUKAWA, T. ISHIKAWA
School of Chemistry, Osaka University of Education, 4-698-1 Asahigaoka, Kashiwara-shi, Osaka-fu 582, Japan

The forced hydrolysis of $FeCl_3$–HCl solution in the presence of surfactants such as sodium dodecyl sulphate (SDS), cetyltrimethyl ammonium chloride (CTAC), polyoxyethylene (20) nonylphenyl ether (NP-20) and poly(oxyethylene–oxypropylene) (PE-64) has been carried out and the precipitated particles were characterized by various techniques. No effect on the morphology of the precipitates was observed for CTAC and NP-20. The addition of a small amount of PE-64 progressed the particle growth but PE-64 yielded small lemon-shape α-Fe_2O_3 particles at high concentration. On the other hand, the morphological uniformity of α-Fe_2O_3 particles was impaired and they changed to needle- or rod-like α-FeOOH particles with increase in the SDS concentration. The α-Fe_2O_3 particles formed with SDS showed a high selective adsorption of H_2O and CO_2, although α-FeOOH particles have no such selectivity. The α-FeOOH particles thus prepared exhibited a low porosity on the heat treatment *in vacuo*.

1. Introduction

The precipitation and characterization of α-Fe_2O_3 particles, uniform in shape and size, have been well studied [1–10]. Previously, we characterized monodispersed spherical and cubic α-Fe_2O_3 particles, produced by a forced hydrolysis of $FeCl_3$–HCl solution, and revealed that these particles were polycrystalline and constructed by an aggregation of fine ferric oxide hydroxide particles [9]. Recently, uniform diamond-shaped and spherical α-Fe_2O_3 particles were also found to be polycrystalline and aggregates [11]. Because the precipitation of metal oxides and hydroxides represents a complex chemical process, the nature of the products may depend in a most sensitive way on the concentration of the reactants, temperature, pH, method of mixing, the kind of anion present, etc. Indeed, the effect of anions in the solution on the morphology and properties of the precipitates is particularly noteworthy. We found marked effects of citrate [12, 13], silicate and phosphate ions [14], formate, lactate, oxalate, tartarate, pyromelate and ethylenediamine tetraacetic acid (EDTA) ions [15], on the formation of α-, β- and γ-FeOOH particles together with the structures and properties of the resulting materials.

We also reported the effects of citrate ions on the formation of α-Fe_2O_3 particles [16]. In addition to these anions, surfactants would be expected to have a strong effect on the formation of colloid particles because they can be highly adsorbed on the nuclei of the precipitating particles. The effects of various kinds of surfactants on the morphology and stability of the metal phosphates [17–23], silver halide [24], gold [25] and ZnO [26] particles have been investigated. However, there is no report on the influence of surfactants on the formation of α-Fe_2O_3 particles. In the present study, therefore, the effects of anionic, cationic, nonionic and copolymer-type surfactants on the formation of α-Fe_2O_3 particles from the forced hydrolysis of $FeCl_3$–HCl solution have been investigated. The properties of the precipitated particles in the presence of SDS will be further discussed in detail.

2. Experimental procedure

2.1. Particle generation and characterization

Sodium dodecyl sulphate (SDS), cetyltrimethyl ammonium chloride (CTAC) and polyoxyethylene (20) nonylphenyl ether (NP-20), were obtained from Wako Co. Ltd, and poly(oxyethylene)oxypropylene (PE-64) was kindly supplied by Sanyo Kasei Corp. PE-46 had the molecular composition $HO(C_2H_4O)_{13}$–$(C_3H_6O)_{30}$–$(C_2H_4O)_{13}$–H. These surfactants were used without further purification. The preparation of α-Fe_2O_3 was done by the same method described in our previous paper [11]; $FeCl_3$–HCl solution with an appropriate amount of surfactants was aged in Teflon-lined screw-capped Pyrex glass vials (30 × 50 mm) at 100 °C for 14 days. The different concentrations of $FeCl_3$ ($\log[FeCl_3] = -2.50$, -2.00 and -1.50) were employed under a fixed concentration of HCl ($\log[HCl] = -2.50$) where the uniform ellipsoidal (~ 40 nm), diamond-shaped (~ 70 nm) and spherical (~ 820 nm) α-Fe_2O_3 particles were produced without surfactants [11]. The concentrations of SDS, CTAC

0022–2461

and NP-20 were varied from 3.16×10^{-4} to 3.16×10^{-2} mol dm^{-3}, whereas that of PE-64 was varied from 0.01–1.0 wt %. For comparison, pure α-FeOOH particles were prepared by adding 1 mol dm^{-3} NaOH solution to 0.1 mol dm^{-3} $Fe(NO_3)_3$ solution up to pH 12 in a polypropylene screw-capped vessel at room temperature [27]. The resulting precipitates were aged at 30 °C and pH 12 for 4 days. All the settled particles thus obtained were thoroughly purified by washing with ion-exchanged and distilled water using a Millipore filter and dried in an air oven at 70 °C for 16 h. The particles so prepared were characterized by transmission electron microscopy (TEM), simultaneous thermogravimetry and differential thermal analysis (TG–DTA), X-ray powder diffraction (XRD) and adsorption of nitrogen at − 196 °C, H_2O at 25 °C and CO_2 at 25 °C as described elsewhere [9].

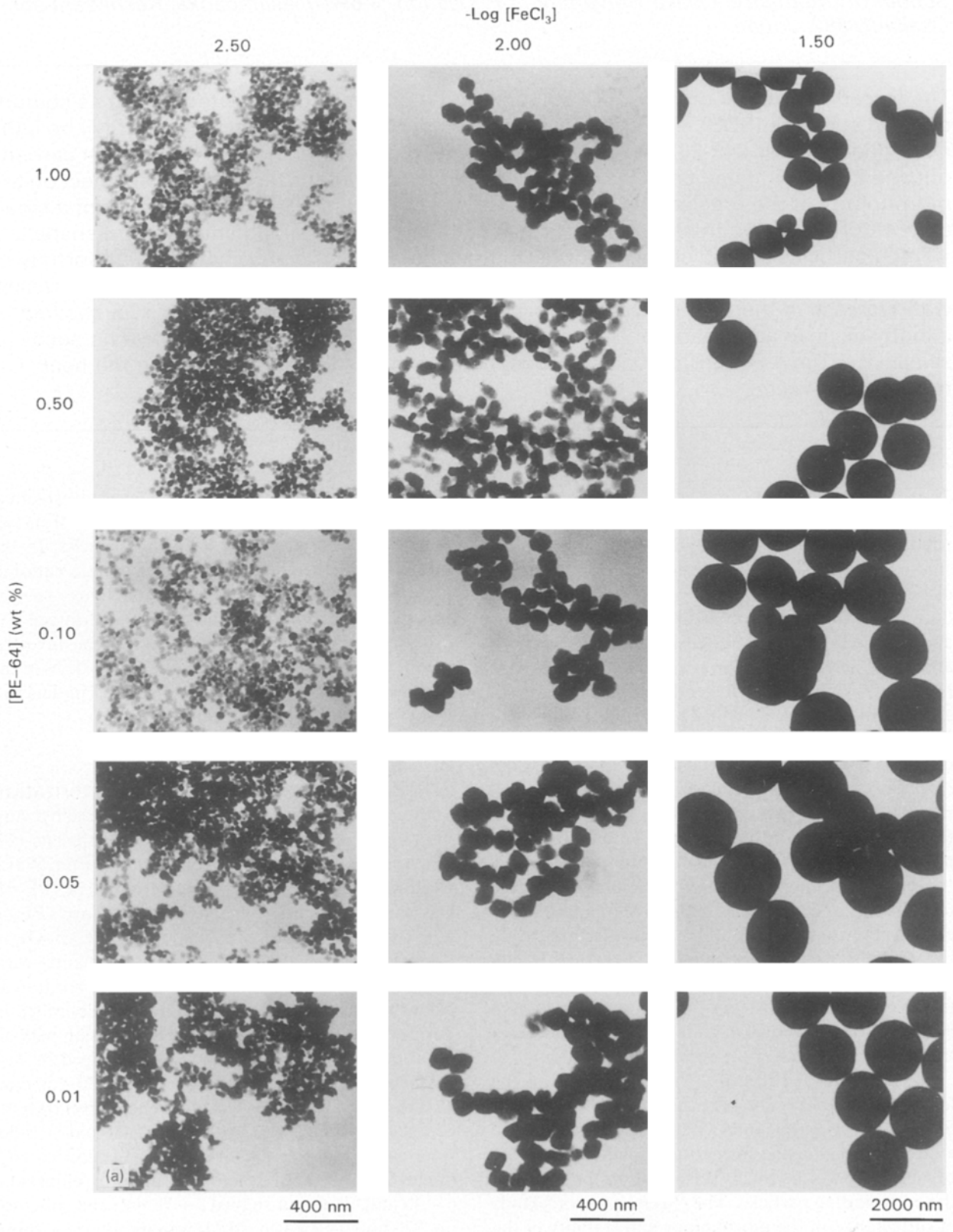

Figure 1 Electron micrographs of the precipitates formed at various concentrations of (a) $FeCl_3$ and PE-64 and (b) $FeCl_3$ and SDS.

3. Results and discussion

3.1. Morphology of precipitated particles

It is clear from TEM observation that the effects of four kinds of surfactants on the shape and size of the precipitated particles markedly differ from one another. The particles precipitated in the presence of NP-20 and CTAC exhibited the same shape and size of the particles produced with or without the respective surfactant, as reported in a previous paper [11], implying no effect of these surfactants on the forced hydrolysis reaction of $FeCl_3$–HCl solution. This result can be reasonably understood because these surfactants have no charge or the same charge as the Fe^{3+} ions. In the case of PE-64 at $\log[FeCl_3] = -1.50$, spherical but rather large particles with a diameter of ~ 1500 nm were formed at [PE-64] = 0.01 wt %. Because the diameter of spherical α-Fe_2O_3 particles produced under the same conditions without surfactants

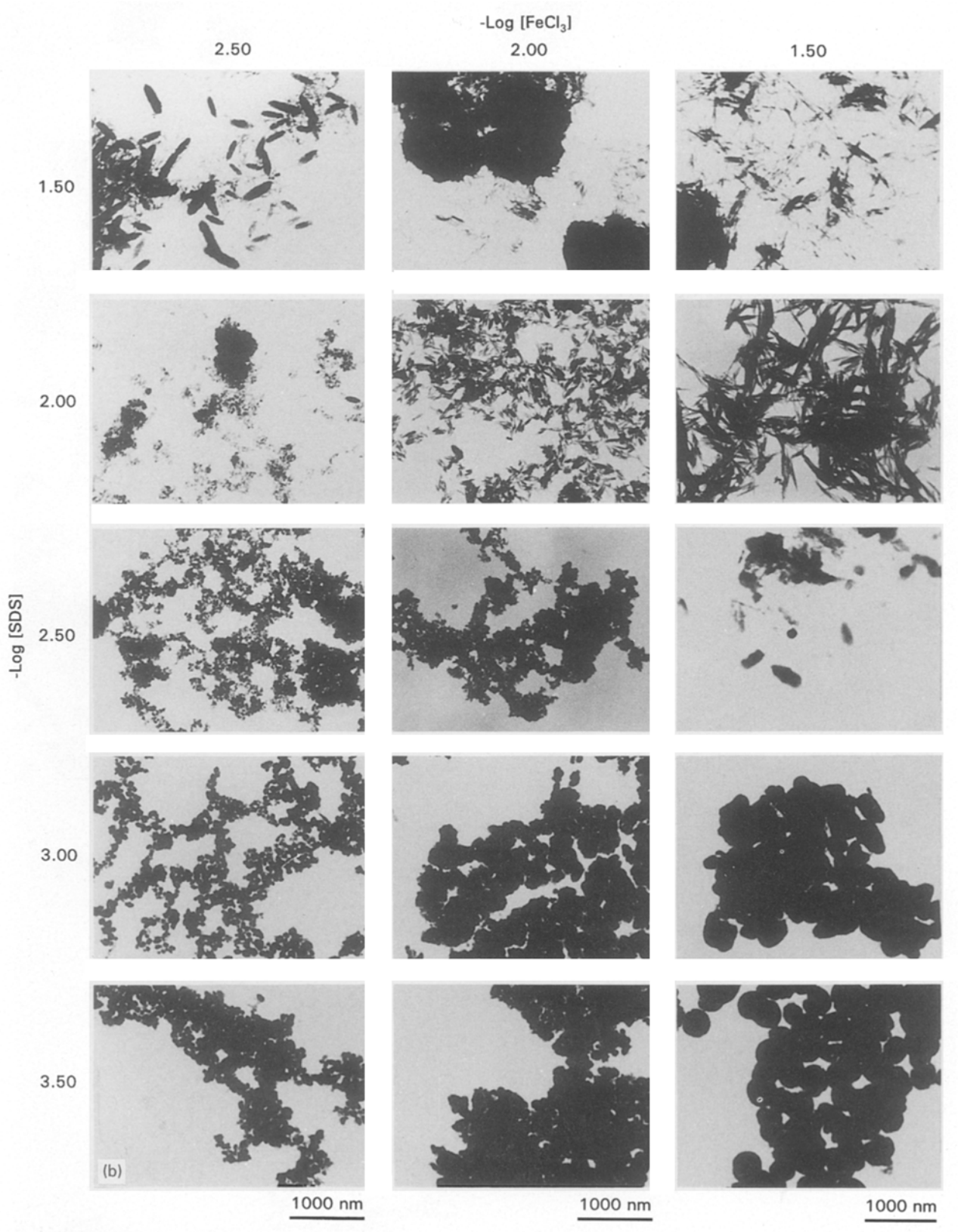

Figure 1 Continued.

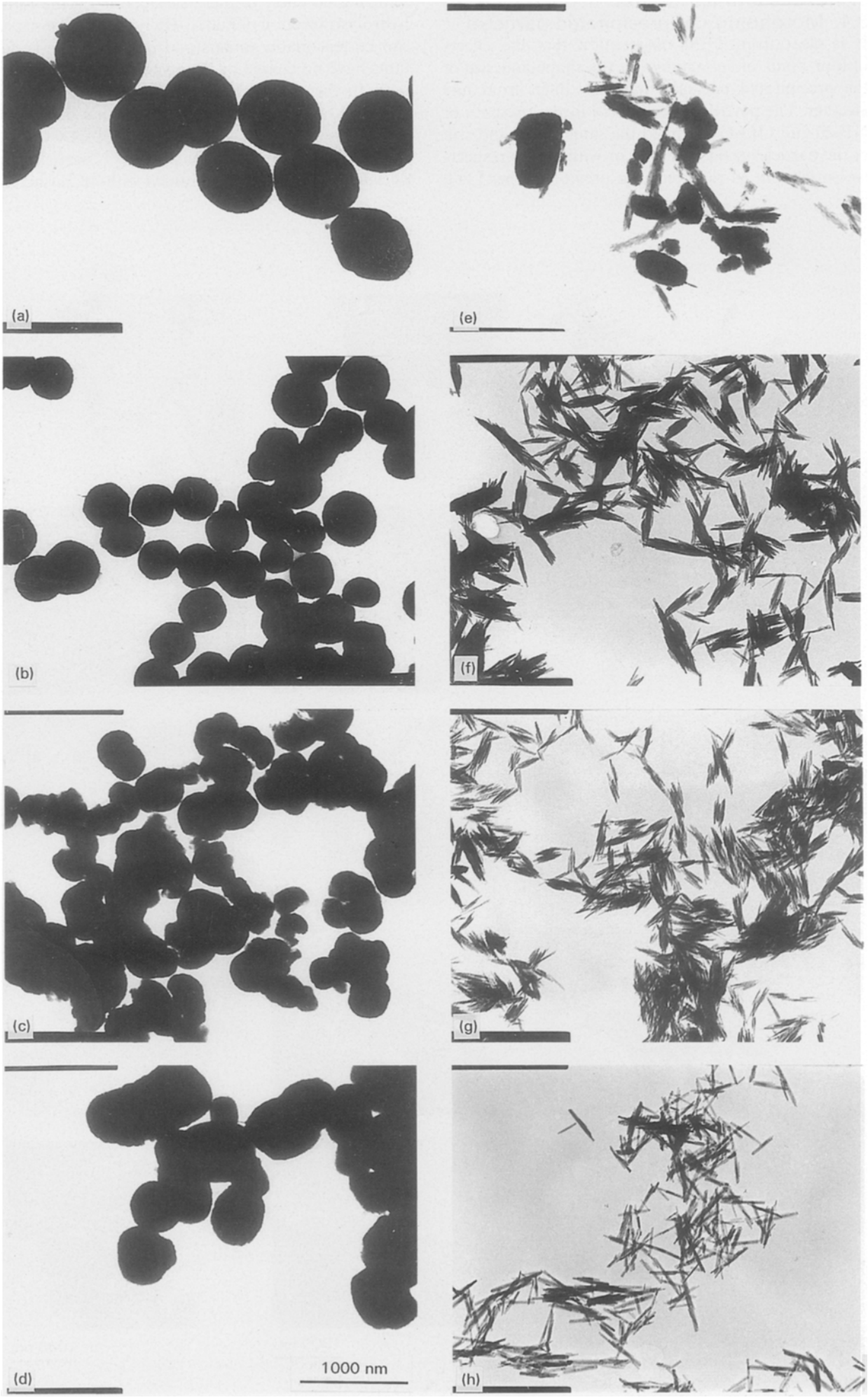
(a)
(b)
(c)
(d)
1000 nm
(e)
(f)
(g)
(h)

is 800 nm [11], it could be considered that a small quantity of PE-64 progressed the particle growth. With increasing concentration of PE-64, the average particle size decreased and finally the particles changed to lemon-shape (~ 800 nm). On the other hand, the morphology and size of the precipitates were dramatically changed with the addition of SDS. At all the $FeCl_3$ concentrations studied, the morphological uniformity of α-Fe_2O_3 particles was impaired and they changed to needle- or rod-like α-FeOOH particles via mixture of these two particles with increasing SDS concentration. The crystal habit of these particles will be discussed later. Fig. 1a and b show typical transmission electron micrographs of precipitated particles for the PE-64 and SDS systems, respectively. Because the particle morphology and crystal habit were remarkably changed for the SDS system, we investigated the effects of SDS in greater detail by varying the concentration of [SDS]/[Fe] (mol %) under a fixed concentration of $FeCl_3$ ($\log[FeCl_3] = -1.50$).

3.2. Characterization of particles precipitated with SDS

Figs 2 and 3 show the transmission electron micrographs and XRD patterns of the particles precipitated in the presence of various amounts of SDS. It is clearly seen in these figures that the uniformity of spherical α-Fe_2O_3 particles was reduced up to 5 mol %, and completely changed to α-FeOOH above 50 mol %. A mixture of α-Fe_2O_3 and α-FeOOH was obtained between 6 and 50 mol %. Additional confirmation on this change of crystal habit on the addition of SDS was given by the Fourier transform–infrared (FT–IR) spectra in KBr (1 wt %) shown in Fig. 4. The intensity of the bands due to the skeleton vibrations of α-Fe_2O_3 at 478 and 572 cm^{-1} decreased with increasing SDS concentration, and new 640, 795 and 895 cm^{-1} bands appeared and developed. The 640 cm^{-1} band was assigned to the deformation vibration of OH^- ions of α-FeOOH and the 795 and 895 cm^{-1} bands to the FeO stretching vibrations [28]. The SDS carries the counter charge to the Fe^{3+} ions, yielding the yellowish precipitates of ferric dodecyl sulphate ($Fe(DS)_3$) above 6 mol % in the starting solution, which coincides with the region of the formation of α-FeOOH. This coincidence strongly implies that the $Fe(DS)_3$ precipitated prior to the hydrolysis reaction acts

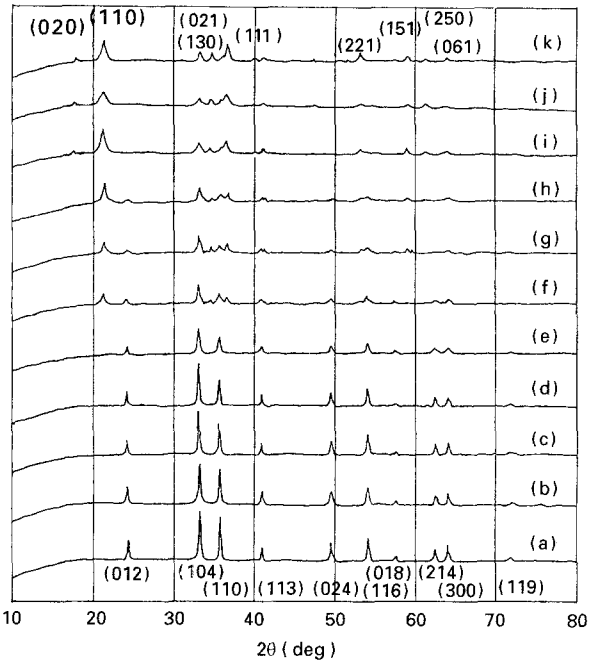

Figure 3 The XRD patterns of precipitates formed at different concentrations of SDS. (a) 0, (b) 1, (c) 3, (d) 5, (e) 10, (f) 15, (g) 20, (h) 30, (i) 50, (j) 100 mol % and (k) pure α-FeOOH.

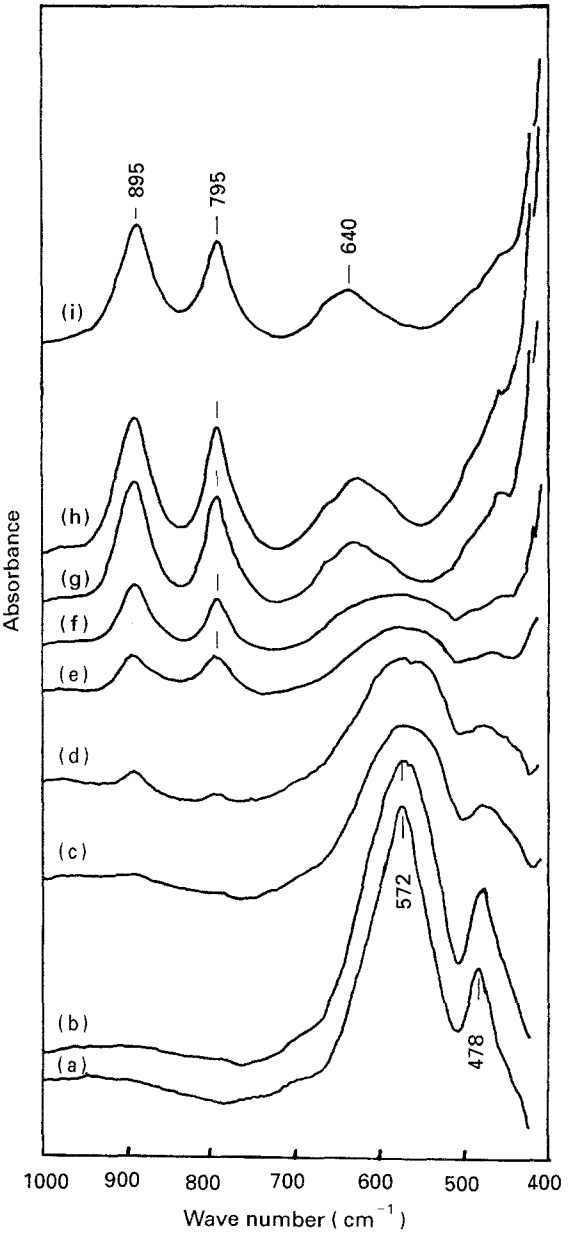

Figure 4 FT–IR spectra of precipitates in KBr (1 wt %) formed in the presence of different concentrations of SDS. (a) 0, (b) 0.8, (c) 5, (d) 10, (e) 15, (f) 30, (g) 50, (h) 100 mol% and (i) pure α-FeOOH.

Figure 2 Electron micrographs of α-Fe_2O_3 particles precipitated at different concentrations of SDS: (a) 0, (b) 0.4, (c) 3, (d) 5, (e) 10, (f) 50, (g) 100 mol % and (h) pure α-FeOOH.

as seeds and/or a precursor of α-FeOOH. Below 5 mol % SDS, however, DS^- ions coordinate with the Fe^{3+} ions and interfere with the hydrolysis and crystal transformation from β-FeOOH to α-Fe_2O_3, resulting in less-crystalline and distorted α-Fe_2O_3 particles.

Fig. 5 shows the TG–DTA curves of the precipitates produced at various SDS concentrations. The characteristic exothermic peaks could be recognized at 150 and 220 °C in the DTA curves and their intensities increased with increasing amount of SDS ions added. These peaks seem to be the decomposition and/or oxidation of the SDS molecules contained in the particles, because a large weight loss occurred around the temperatures of these two peaks.

Table I summarizes the results of chemical analyses, together with the relevant gas adsorption information. The concentrations of SDS and iron in the particles were assayed, respectively, by inductively coupled plasma (ICP) measurement and carbon, hydrogen and nitrogen elemental analysis. It is noticeable in Table I that the [SDS]/[Fe] mol % in α-Fe_2O_3 particles is appreciably equivalent to that in the starting solution, implying that the added SDS molecules are incorporated in the particles, in agreement with the result of TG–DTA measurement. To characterize the surface and inner structure of precipitated particles, we employed gas adsorption and FT–IR measurements, as described below. The adsorption isotherms of nitrogen and H_2O showed the Type II isotherm of Brunaver-Deming-Deming-Teller (BDDT) classification while those of CO_2 showed Langmuir type. Hence, the monolayer adsorption capacities of nitrogen, H_2O and CO_2 on the particles were evaluated, respectively, by applying the BET andLangmuir equations, and the specific surface area of the particles from these adsorptives (abbreviated A_n, A_w and A_c, respectively) were calculated by assuming the cross-sectional areas of these adsorptive molecules to be 0.162, 0.108 and 0.206 nm^2, respectively [29]. The calculated A_n, A_w and A_c values are given in Table I.

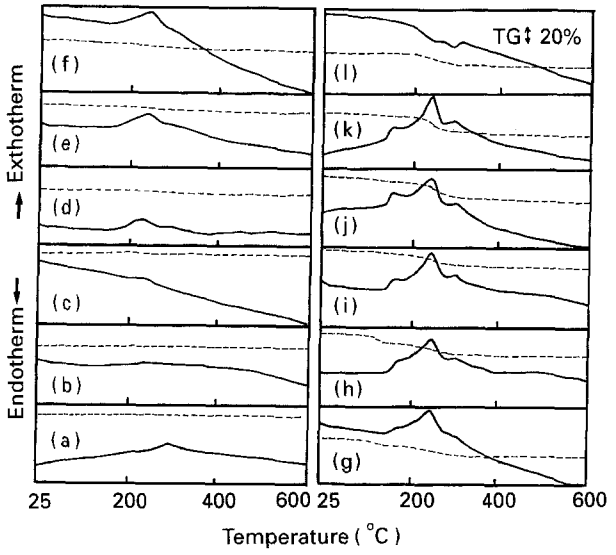

Figure 5 TG–DTA curves of precipitates formed in the presence of different concentrations of SDS. (—) DTA and (– – –) TG curves. (a) 0, (b) 0.6, (c) 1, (d) 3, (e) 5, (f) 10, (g) 15, (h) 20, (i) 30, (j) 50, (k) 100 mol % and (i) pure α-FeOOH.

Fig. 6 plots A_n, A_w/A_n and A_c/A_n as a function of the amounts of SDS added in the starting solution. The A_n values of α-Fe_2O_3 decreased from 20 to less than 1 $m^2 g^{-1}$ on increasing the SDS concentration up to 5 mol %, while α-FeOOH produced above 50 mol % exhibited high A_n values. It should be emphasized that A_w/A_n and A_c/A_n were maximum at 3 mol %, whilst they approximated unity above 50 mol %. Because these ratios are a measure of the selective adsorption of H_2O and CO_2, these results strongly show that α-Fe_2O_3 produced in the presence of 3 mol % SDS has a high selectivity in H_2O and CO_2 adsorption, whereas α-FeOOH formed above 50 mol % SDS has no such selectivity.

The diameters of the H_2O, nitrogen and CO_2 molecules estimated from their second virial coefficients are 0.276, 0.353 and 0.440 nm, respectively. Comparing the molecular size, the molecular sieve effect of the pores in the particles cannot interpret this high selectivity of gas adsorption, therefore we should consider the polarity of the adsorptive gas molecules. The polar molecules should induce a higher chemical affinity for the SDS molecules contained in the particles, as was

TABLE I The results of chemical analyses and specific surface areas of the particles precipitated at different concentrations of SDS measured by $N_2(A_n)$, $H_2O(A_w)$ and $CO_2(A_c)$ adsorption

SDS/Fe (mol %)		n_s^a (mol nm^{-2})	A_n^b ($m^2 g^{-1}$)	A_w^b ($m^2 g^{-1}$)	A_c^b ($m^2 g^{-1}$)
Solution	Solid				
α-Fe_2O_3					
0	0	0	19.5	31.2	40.8
1	1.4	1.0	7.8	36.0	36.5
2	3.2	4.9	3.7	54.2	35.9
3	3.1	56.4	0.4	62.2	48.1
4	5.1	52.2	0.6	59.0	48.0
5	6.8	51.4	0.8	58.8	46.3
α-FeOOH					
50	5.8	0.6	53.2	68.2	24.4
100	12.2	1.1	61.7	69.9	32.7
Pure	–	–	75.3	80.0	68.8

[a] Number of SDS molecules on unit surface area of particles.
[b] Samples were outgassed at 100 °C.

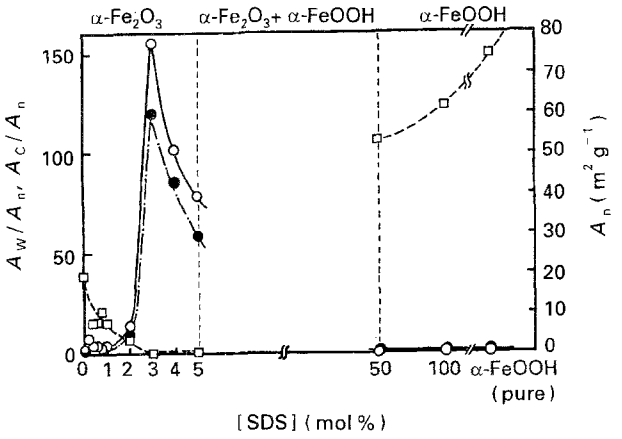

Figure 6 Change in A_n, A_w/A_n and A_c/A_n values of the precipitates formed at different concentrations of SDS. (□) A_n, (○) A_w/A_n, (●) A_c/A_n.

ascertained by the TG–DTA, ICP and elemental analysis measurements (Table I). To speculate the state of SDS in the particle, the number of SDS molecules on a unit surface area of the samples, n_s, was calculated by assuming all SDS molecules to exist on the particle surface, and is given in Table I. As can be seen in Table I, large n_s values above 50 mol nm^{-2} are found for particles prepared in the presence of 3–5 mol % SDS. Taking the cross-sectional area of the SDS molecule to be 0.21 nm^2 [30], n_s should be 4.8. The large n_s for the α-Fe_2O_3 particles which show a high selective adsorption of H_2O and CO_2 strongly implies that the SDS molecules exist not only in the surface layer of the particles but also in the bulk phase. This result suggests that polar H_2O molecules penetrate into the α-Fe_2O_3 particles and coordinates to form Fe–DS complexes or SDS molecules. This adsorption behaviour was evinced by the large hysteresis loops observed on five cycles of adsorption–desorption isotherms. However, every cycle provided the same isotherm and closed at zero relative pressure on prolonged evacuation, indicating that H_2O molecules are physically adsorbed.

The pure α-FeOOH particle transformed to α-Fe_2O_3 when treated above 200 °C *in vacuo*, while the α-FeOOH produced with 100 mol % SDS was changed to Fe_3O_4 above 200 °C *in vacuo*. The combustion of SDS molecules in the particles could consume oxygen to reduce the α-Fe_2O_3 to Fe_3O_4. A more interesting difference between these two α-FeOOH particles was observed in the dependence of A_n on the pretreatment temperature, as shown in Fig. 7. A_n rapidly increased up to 300 °C with increasing porosity, but dropped at 400 °C for the pure α-FeOOH particles, whilst A_n of the α-FeOOH particles produced with 100 mol % SDS changed slightly between 62 and 88 $m^2 g^{-1}$. This temperature dependence of the latter α-FeOOH particles suggests that SDS molecules would progress the crystal growth of the α-FeOOH particle to give a high crystallinity, although no difference in crystallinity between pure and SDS-containing α-FeOOH particles was detected by the XRD measurement. The reason for this is not clear at present, but it should shed more light on these interesting phenomena.

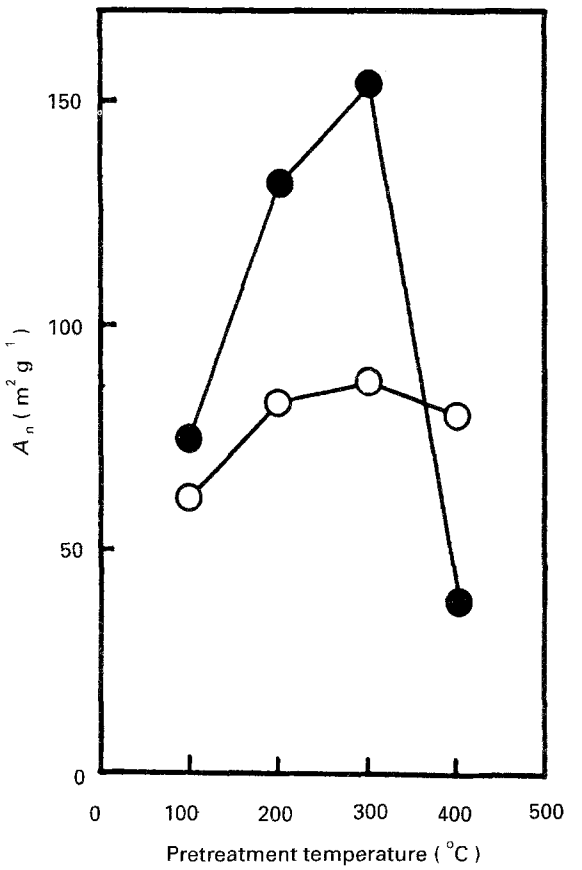

Figure 7 Change in A_n of α-FeOOH with pretreatment temperature. (●) pure α-FeOOH, (○) α-FeOOH precipitated at 100 mol % SDS.

Acknowledgements

The authors thank Dr Yoshihira Okanda and Dr Masao Fukusumi, Osaka Municipal Technical Research Institute, for help with the transmission electron microscope measurements.

References

1. E. MATIJEVIĆ, *Langmuir* **2** (1986) 12.
2. *Idem, Ann. Rev. Mater. Sci.* **15** (1985) 483.
3. E. MATIJEVIĆ and P. SCHEINER, *J. Coll. Interface Sci.* **63** (1978) 509.
4. N. KALLY and E. MATIJEVIĆ, *Coll. Surf.* **13** (1985) 45.
5. E. MATIJEVIĆ and S. CIMAS, *Coll. Polym. Sci.* **265** (1987) 155.
6. S. HAMADA, S. NIIZEKI and Y. KUDO, *Bull. Chem. Soc. Jpn* **59** (1986) 3443.
7. S. HAMADA and E. MATIJEVIĆ, *J. Chem. Soc. Farad. Trans. 1* **78** (1982) 2174.
8. U. SCHWERTMANN and R. M. CORNELL, "Iron Oxides in the Laboratory" (VCH, New York, 1991).
9. K. KANDORI, Y. KAWASHIMA and T. ISHIKAWA, *J. Chem. Soc. Farad. Trans.* **87** (1991) 2241.
10. *Idem, J. Mater. Sci. Lett.* **12** (1993) 288.
11. J. KANDORI, S. TAMURA and T. ISHIKAWA, *Coll. Polym. Sci.* **272** (1994) 812.
12. K. KANDORI, M. FUKUOKA and T. ISHIKAWA, *J. Mater. Sci.* **26** (1991) 3313.
13. T. ISHIKAWA, H. NISHIMORI, I. ABE and K. KANDORI, *Coll. Surf.*, in press.
14. K. KANDORI, S. UCHIDA, S. KATAOKA and T. ISHIKAWA, *J. Mater. Sci.* **27** (1992) 719.
15. T. ISHIKAWA, S. KATAOKA and K. KANDORI, *ibid.* **28** (1993) 2693.
16. K. KANDORI, Y. KAWASHIMA and T. ISHIKAWA, *J. Coll. Interface Sci.* **152** (1992) 284.

17. T. ISHIKAWA and E. MATIJEVIĆ, *ibid.* **123** (1988) 122.
18. K. KANDORI, M. TOSHIOKA, H. NAKASHIMA and T. ISHIKAWA, *Langmuir* **9** (1993) 1031.
19. L. L. SPRINGSTEEN and E. MATIJEVIĆ, *Coll. Polym. Sci.* **267** (1989) 1007.
20. R. B. WILHELMY and E. MATIJEVIĆ, *Coll. Surfaces* **22** (1987) 111.
21. E. P. KATSANIS and E. MATIJEVIĆ, *ibid.* **5** (1982) 43.
22. K. KANDORI, H. NAKASHIMA and T. ISHIKAWA, *J. Coll. Interface Sci.* **160** (1993) 499.
23. T. ISHIKAWA and E. MATIJEVIĆ, *Coll. Polym. Sci.* **269** (1991) 179.
24. E. MATIJEVIĆ and R. H. OTTEWILL, *J. Coll. Sci.* **13** (1958) 242.
25. S. KANEKO, T. TORIGOE and K. ESUMI, *Shikizai* **66** (1993) 14.
26. A CHITTOFRATI and E. MATIJEVIĆ, *Coll. Surfaces* **48** (1990) 65.
27. T. ISHIKAWA, S. NITTA and S. KONDO, *J. Chem. Soc. Farad. Trans. 1* **82** (1986) 2401.
28. W. B. WHITE and R. ROY, *Am. Mineral.* **49** (1964) 1670.
29. S. J. GREGG and K. S. W. SING, "Adsorption, Surface Area and Porosity" (Academic Press, London, 1982).
30. C. TANFORD, "The hydrophobic effect: Formation of Micelles and Biological Membranes" (Wiley Interscience, New York, 1980) p. 56.

Received 29 July 1993
and accepted 8 September 1994